 MCB, vol.8, no.2, pp.105-122, 2011

A Continuum Model for Pressure-Flow Relationship in Human Pulmonary Circulation

Wei Huang[*,†], **Qinlian Zhou**[†,‡], **Jian Gao**[‡] **and R. T. Yen**[‡,§ ¶]

Abstract: A continuum model was introduced to analyze the pressure-flow relationship for steady flow in human pulmonary circulation. The continuum approach was based on the principles of continuum mechanics in conjunction with detailed measurement of vascular geometry, vascular elasticity and blood rheology. The pulmonary arteries and veins were considered as elastic tubes and the "fifth-power law" was used to describe the pressure-flow relationship. For pulmonary capillaries, the "sheet-flow" theory was employed and the pressure-flow relationship was represented by the "fourth-power law". In this paper, the pressure-flow relationship for the whole pulmonary circulation and the longitudinal pressure distribution along the streamlines were studied. Our computed data showed general agreement with the experimental data for the normal subjects and the patients with mitral stenosis and chronic bronchitis in the literature. In conclusion, our continuum model can be used to predict the changes of steady flow in human pulmonary circulation.

Keywords: continuum model, pulmonary circulation, pressure-flow relationship, capillary sheet, steady flow.

1 Introduction

Pulmonary blood vessels are consistently subjected to mechanical stimuli, including the stretch and shear stress resulting from circulatory pressure and flow, modulate vascular functions by activating mechanosensors, signaling pathways, and gene and protein expressions [Chien (2007)]. The pressure-flow relationship of pulmonary circulation is extremely important to the understanding of the diseases

[*] Department of Health Technology and Informatics, The Hong Kong Polytechnic University, Kowloon, Hong Kong

[†] Wei Huang and Qinlian Zhou contributed equally to this work.

[‡] Dept. of Biomedical Engineering, The University of Memphis, Memphis, TN 38152

[§] Correspondent author. E-mail: myen@memphis.edu.

[¶] This paper is a tribute to Prof. Pin Tong in honor of his 72th birthday, and edited by Dr. David Lam.

of the lung and heart [Yuan, Garcia, Hales, Stuart, Archer and West (2010)]. A thorough theoretical understanding with full experimental verification is essential. Two general theoretical approaches have been used: One is the electric circuit analog, or the "lumped parameter" model, the other is biomechanical approach, or the "continuum" model.

For the "lumped parameter" models, it is difficult to attach physiological significance to the parameters used in the models because anatomic details are ignored [Westerhof, Stergiopulos and Noble (2004)]. Whereas the lumped parameter approach is often convenient and effective, the continuum approach is more fundamental because it is based on the principles of continuum mechanics in conjunction with detailed measurement of vascular geometry, vascular elasticity and blood rheology. In the continuum approach, the vessels are classified into different orders with a separate set of parameters for each order. The principles of continuum mechanics are employed to derive the pressure-flow relationship in the vessel tubes and the capillary bed. Equations for arteries and veins of all orders as well as equations for the capillary bed are then concatenated in sequence to complete the circulation circuit. Flow and pressure distributions can be obtained by solving the equations sequentially. Therefore, the continuum approach provides an analytical tool to analyze the physiological problems, and to synthesize the many components of a complex problem so that quantitative predictions are made possible.

A continuum model for steady blood flow in cat lung was successfully developed by [Zhuang, Fung and Yen (1983)]. In the calculations, the sheet flow theory of Fung and Sobin (1969) is used for pulmonary capillary blood flow and an analogous "fifth power" is used for flow in the arteries and veins. Later on, Yen and Sobin (1988) performed experiments which validated the theoretical predictions in a general agreement. Gan and Yen (1994) used the continuum approach to analyze vascular impedance in dog lungs. However, similar analysis for human lungs has been lacking. In this paper, a continuum model for steady flow in human pulmonary circulation was studied.

2 Methods

2.1 Mathematical approach of pressure-flow analysis

The mathematical approach of pressure-flow analysis used in this work is similar to that of Zhuang, Fung and Yen (1983). A brief description is given below. It was shown that for pulmonary arteries and veins, the vessel diameter D changes linearly with the appropriate transmural pressure ΔP,

$$\frac{D}{D_0} = 1 + \beta \Delta P. \tag{1}$$

Here D_0 is the tube diameter when transmural pressure is zero and β is the compliance coefficient of the vessel wall defined by Yen, Fung and Bingham (1980). Then for a viscous incompressible fluid in a circular vessel, the steady flow is governed by Poiseulle's law and can be presented as

$$\frac{640\mu\beta D_0 L}{\pi}\dot{Q} = D_0^5\left[(1+\beta\Delta P_{entry})^5 - (1+\beta\Delta P_{exit})^5\right], \tag{2}$$

where μ is the apparent viscosity of blood, L is the length of the vessel, $\dot{Q}$ is the flow rate in the vessel, ΔP_{entry} and ΔP_{exit} are transmural pressures at the entry and exit ends of the vessel. This is called the fifth power law.

When applying the fifth power law in computation, ΔP is calculated as follows [Yen, Fung and Bingham (1980)]. For pulmonary vessels with diameters much larger than the alveolar diameter,

$$\Delta P = P - P_{pl}, \tag{3}$$

whereas for vessels with diameters smaller than the alveolar diameter,

$$\Delta P = P - P_A. \tag{4}$$

Here, P is blood pressure, P_A is airway pressure and P_{pl} is pleural pressure.

In [Zhuang, Fung and Yen (1983)], losses due to turbulence and bifurcation were accounted for, as well as the effect of change in kinetic energy along the stream. In our model, these factors are ignored since the Reynolds number is very small (the main pulmonary artery has the largest value, which is 464) and the static pressure drop at the junction caused by change in kinetic energy is in the order of magnitude of 10^{-2} cm H_2O.

According to the sheet flow theory [Fung and Sobin (1969)], the dense network of capillary blood vessels in pulmonary alveolar wall is modeled as a sheet of fluid flowing between two membranes held apart by a large number of regularly spaced posts. If the local blood pressure is larger than the alveolar gas pressure, then the sheet thickness can be computed as

$$h = h_0 + \alpha(P - P_A) \tag{5}$$

where h is the sheet thickness, h_0 is the thickness of capillary sheet at zero pressure difference when the pressure decreases from positive values, α is the compliance constant of the capillary sheet, P is blood pressure and P_A is airway pressure.

Based on Eq. (5), the pressure-flow relationship in capillary sheet is represented as [Fung and Sobin (1972)]

$$\dot{Q} = const\left(h_a^4 - h_v^4\right) = const\left\{\left[h_0 + \alpha\left(P_{art} - P_A\right)\right]^4 - \left[h_0 + \alpha\left(P_{ven} - P_A\right)\right]^4\right\}. \quad (6)$$

Here $\dot{Q}$ is the volume flow rate, h_a is the sheet thickness at the arteriole end, h_v is the sheet thickness at the venule end, and P_{art} and P_{ven} are pressures at the corresponding arteriole and venule. The constant *const* equals to

$$const = \frac{SA}{4\mu k f \bar{L}^2 \alpha}, \quad (7)$$

where A is alveolar area, S is the vascular-space-tissue ratio, representing the fraction of the blood volume over a sum of the volumes of the vascular space and the posts. μ is the apparent viscosity of blood in the capillary sheet. k and f are dimensionless factors which describe alveolar structural geometry. $\bar{L}$ is the average length of streamlines between an arteriole and a venule, or the average length of capillaries. Zhong, Dai, Mei and Tong (2002) presented a micromechanical theory of flow in pulmonary alveolar sheet.

Equations (5) and (6) are valid only when $P_{ven} \geq P_A$. If $P_{ven} < P_A$, it is said to be in zone 2 condition and "waterfall" occurs. The sluicing gate is located at the junction of the capillary sheet and its draining venule. Hence in zone 2 condition h_v tends to 0, and the flow depends only on h_a.

A repeated application of Eq. (2) to each order of arteries and veins as well as the application of Eq. (6) to the capillary sheet made a complete pulmonary circulation system.

2.2 Morphometric and elastic property of human lung

Morphometric information of the human pulmonary arteries and veins contains vessel diameter, length, and branching pattern. Based on the measurements of the silicone elastomer casts of human lungs, Huang, Yen, McLaurine and Bledsoe (1996) constructed a vessel branching system that consists of 15 orders of arteries between the main pulmonary artery and capillary sheet and 15 orders of veins between the capillary sheet and left atrium. Since the vessels of the same order were considered to be parallel, we used the diameter and length of elements, not segments, of arteries and veins [Huang, Yen, McLaurine and Bledsoe (1996)]. The diameter and length of the main pulmonary artery in [Singhal, Henderson, Horsfield, Harding and Cumming (1973)] were used. Other information for vessels included apparent viscosity [Yen and Fung (1973)] and compliance [(Yen and Sobin (1988); Yen, Tai,

Table 1: Morphometry and elasticity data of human pulmonary veins[#]

Order	Number of Branches, Nn	Diameter D_0n (cm)	Length Ln (cm)	Apparent Viscosity, μ (cP)	Compliance β
15	4	1.2970	3.5680	4.0	0.708*
14	8	0.8650	3.4990	4.0	0.708*
13	22	0.5860	1.9490	4.0	0.708*
12	62	0.4000	2.6490	4.0	0.708*
11	126	0.2880	1.7900	4.0	0.708*
10	286	0.1990	1.4780	4.0	0.708*
9	870	0.1420	1.1240	4.0	0.708*
8	2134	0.0900	0.6780	4.0	0.708†
7	7442	0.0620	0.4790	4.0	0.887†
6	31134	0.0380	0.2920	4.0	1.260†
5	146050	0.0230	0.1500	4.0	1.260†
4	906102	0.0130	0.1060	4.0	1.798†
3	4332666	0.0067	0.0380	3.5	0.433‡
2	16988490	0.0031	0.0210	3.0	0.625‡
1	79647106	0.0018	0.0130	2.5	1.010‡

[#]: at P_A-P_{pl} = 10 cm $H_2O cm H_2O$. *: Unknown compliance coefficients obtained by extrapolating from the nearest order of vessels. †: data from Yen, Tai, Rong, and Zhang (1990). ‡: data from Yen and Sobin (1988).

Rong and Zhang (1990)]. The morphometric and elasticity data of pulmonary veins and arteries used in our model are summarized in **Table 1** and **Table 2**, respectively.

There were no experimental data in the literature for the elasticity of arteries of order 4 and 5, arteries from orders 11 to 14, and veins from orders 9 to 15. The data we used in this work were obtained by extrapolating the nearest vessel order. It will be shown later that this kind of approximation is acceptable because variation of vessel elasticity data will not cause significant change in pressure-flow relationship.

In human pulmonary vasculature, a larger artery (of order 16 to 7) would branch into more than 5 daughter branches with different orders [Huang, Yen, McLaurine and Bledsoe (1996)]. For such a system, it was not theoretically feasible to account for the asymmetric branching pattern since the pulmonary circulation system was not considered as a distributed network in our model. Hence the simplest approximation was used: the vessels of different orders were linked in series and the vessels of the same order were considered as parallel and treated identically. Flow in a larger vessel was equally distributed into its daughter vessels and all vessels of

Table 2: Morphometry and elasticity data of human pulmonary arteries[#]

Order	Number of Branches, Nn	Diameter D_0n (cm)	Length Ln (cm)	Apparent Viscosity, μ (cP)	Compliance β
1	102411624	0.0020	0.0220	2.5	0.698‡
2	28114394	0.0036	0.0260	3.0	0.482‡
3	10203806	0.0056	0.0360	3.5	0.361‡
4	4513692	0.0097	0.0450	4.0	0.361*
5	1348338	0.0150	0.0680	4.0	0.361*
6	571544	0.022	0.108	4.0	1.135†
7	172040	0.034	0.192	4.0	0.932†
8	44008	0.051	0.281	4.0	0.877†
9	12450	0.077	0.373	4.0	1.238†
10	3448	0.116	0.658	4.0	1.281†
11	900	0.175	1.235	4.0	1.281*
12	254	0.271	1.807	4.0	1.281*
13	86	0.416	2.597	4.0	1.281*
14	14	0.734	3.569	4.0	1.281*
15	4	1.480	2.53	4.0	1.281*
16	1	3.0 [19]	9.05 [19]	4.0	1.281*

[#]: at P_A-P_{pl} = 10 cm $H_2O cmH_2O$. *: Unknown compliance coefficients obtained by extrapolating from the nearest order of vessels. †: data from Yen, Tai, Rong and Zhang (1990). ‡: data from Yen and Sobin (1988).

the same order had the same flow rate and pressure drop.

The variation of the apparent viscosity of blood in the pulmonary capillary sheet with hematocrit was determined by Yen and Fung (1973) in model experiments. The apparent viscosity was approximately 1.92 cp when the hematocrit was 30%. The apparent viscosity was assumed to be 4.0 cp in larger vessels in their model. Then the apparent viscosity of blood in small vessels of the orders of 1-3 was estimated by linear interpolation as 2.5, 3.0, and 3.5, respectively, as shown in **Tables 1** and **2**.

Table 3 summarizes a set of parameters for capillary sheet used in our computation and the literature where those data were reported.

Since the data of the average length of capillaries, $\bar{L}$ in human lung was not available we estimated it based on the ratio of the alveolar diameter D of human (age: 8∼74 yr.), dog, and cat = 250: 94: 117 [Altman and Dittmer (1971)]. Sobin, Fung, Lindal, Tremer and Clark (1980) found that in cat lungs the average length

Table 3: Morphometry, elasticity and blood viscosity data of the capillary sheet

Symbol	Value	Reference
h_0	3.5 μm	Sobin, Fung, Tremer and Lindal (1979)
α	0.127 $\mu m/cmH_2O$	Sobin, Fung, Tremer and Lindal (1979)
$\bar{L}$	1188 μm	See text
S	0.88	Sobin, Fung, Tremer and Lindal (1979)
A	126 m^2	Gehr, Bachofen and Weibel (1978)
μ	1.92 cP	Yen and Fung (1973)
K	12	Fung (1972)
F	1.8	Lee (1969)

of capillaries $\bar{L}$ = 556 $\pm$ 286 μm. Gan and Yen (1994) estimated that in dog lungs $\bar{L}$= (94$\times$556)/117 = 447 μm. In this study, we estimated in human lung $\bar{L}$ = (250$\times$556)/117 = 1188 μm.

3 Results

Figure 1 shows the relationship between flow rate and pulmonary arterial pressure in six different conditions. In the three cases of positive inflation, pleural P_{pl} was 0, left atrial pressure P_v was fixed at 3 cmH_2O and airway pressure P_A was indicated in **Figure 1**. In the other three cases of negative inflation, P_{pl} was indicated in the figure, P_A was 0, and P_v was 2 cmH_2O. The curves show that the pressure-flow relationship was nonlinear. Flow $\dot{Q}$ increased much faster than arterial pressure P_a did. Resistance to blood flow was higher in positive inflation than in negative inflation. In the cases of positive inflations, resistance increased with increasing transpulmonary pressure; whereas in negative inflations, resistance decreased with increasing transpulmonary pressure, although the effect was insignificant. Compared to the data reported in animal study [Zhuang, Fung and Yen (1983)], the flow rate in human lung was higher than that in cat lung at the same pulmonary arterial pressure level.

As shown in the curves for positive inflation where airway pressure was 7 cm H2OcmH_2O, there was a change at the point where flow rate was about 50 ml/s. That was the point where the condition changed from zone 3 to zone 2, causing a slight variation in pressure-flow relationship.

As mentioned earlier, the elasticity data of certain orders of arteries and veins were lacking. The sensitivity of our model to the changes of elasticity data was therefore tested. Values of compliance for all vessels were changed and the resulting longitudinal pressure distribution was calculated. As shown in **Figure 2**, when elasticity

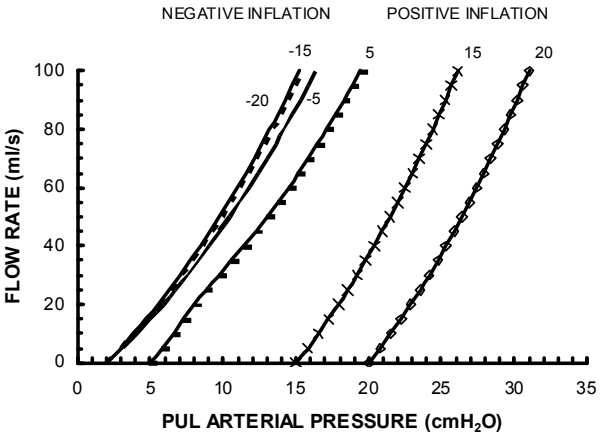

Figure 1: Relationship between flow rate and pulmonary arterial pressure under six different transpulmonary pressures. In positive inflations, airway pressure was indicated in the figure while pleural pressure was fixed at 0 and left atrial pressure at 3 cm $H_2O cmH_2O$; in negative inflations, airway pressure was 0, pleural pressure was indicated in the figure while left atrial pressure is fixed at 2 cm $H_2O cmH_2O$.

data of all vessels were decreased to half of their regular value, pressure increased by a small amount (with 7.4% increment at the main pulmonary artery).

When elasticity data of all vessels were increased to 1.5 times of the regular value, pressure decreased by a small amount (with 5.4% decrement at the main pulmonary artery). If we only changed the elasticity data of vessel orders for which no measurement was available, the effect on pressure distribution was even smaller and hence the error caused by inaccurate elasticity data can be neglected.

Local regulation of pulmonary blood pressure is believed to be accomplished by vasoconstriction of muscular arteries (diameter range 50-500 μm [Wagenvoort and Wagenvoort (1977)], order 3-8). This was well demonstrated in our model. **Figure 3** shows the longitudinal pressure distributions at three levels of lumen diameter of muscular arteries: 50% constriction, regular, and 50% dilation.

As shown in **Fig. 3**, the constriction of muscular arteries caused dramatic increase in pulmonary arterial pressure, while vessel dilation did not yield significant change in arterial pressure.

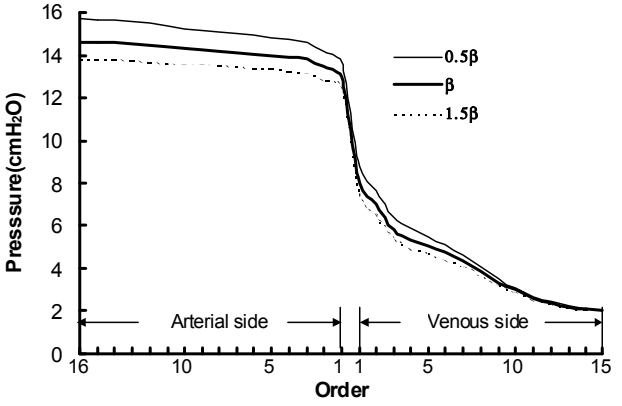

Figure 2: Effects of changing elasticity data on longitudinal pressure distributions. Three sets of elasticity data were used: regular value as listed in **Table 1** and **Table 2**, half of regular value, and 1.5 times of regular value. For all cases, P_A = 0 cm $H_2O cmH_2O$, P_{pl} = -5 cm $H_2O cmH_2O$, P_v = 2 cm $H_2O cmH_2O$.

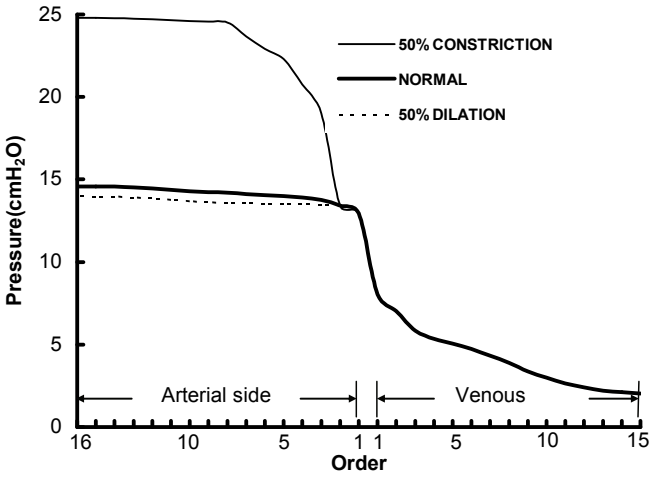

Figure 3: Effects of vasoconstriction on longitudinal pressure distributions. Three sets of lumen diameter data of muscular arteries were used: regular value as listed in **Table 2**, half of regular value, and 1.5 times of regular value. For all cases, P_A = 0 cm $H_2O cmH_2O$, P_{pl} = -5 cm $H_2O cmH_2O$, P_v = 2 cm $H_2O cmH_2O$.

4 Discussion

For studies in normal subjects at rest or during exercise, Fowler (1969) concluded that the relationship between pulmonary arterial pressure and flow was linear if mean value of several subjects was used, although considerable individual variation did exist. He also mentioned that comparing the values during exercise to those at rest, the percentage increment of pressure was generally less than that of blood flow, indicating no rise of pulmonary vascular resistance with increasing blood flow. Harris, Segel and Bishop (1968) examined the passive relation between pressure and flow by occlusion of the right pulmonary artery. They tested three groups of subjects: normal subjects, patients with mitral stenosis and patients with chronic bronchitis. For each subject, four data points were obtained: at rest with balloon deflated, at rest with balloon inflated, after exercise with balloon deflated and after exercise with balloon inflated. Compared to other reports [Fowler (1969); Janicki, Weber, Likoff and Fishman (1985); Kussmaul, Wieland and Laskey (1988); Laskey, Ferrari, Palevsky and Kussmaul (1993); Luchsinger, Sachs and Patel (1962); Seibold, Wieshammer and Kress (1988)], Harris, Segel and Bishop (1968) provided two more points of pressure-flow data sets, which made it a better validation for our model. For normal subjects, as shown in **Table 4**, our computed date agreed with the experimental data in general.

In our calculation, P_A = 0 cm $H_2O cm H_2O$, P_{pl} = -5 cm $H_2O cm H_2O$ and P_v equal to wedge pressure from experiments were used. In cases where the balloon was inflated, we doubled the value of blood flow listed in the table and used the result as flow input for the model, assuming half of the blood flow through left lung. The same values of vessel compliance were used whether the patient was at rest or after exercise, which indicated that exercise did not cause significant changes in the mechanical properties of the vessels. All computed results were very close to the experimental data except in two cases: patient N2 and N3 during exercise with balloon inflated. For patient N2, if we introduced a 36% constriction of lumen diameter to muscular arteries (order 3-8), we got a pulmonary arterial pressure (PAP) of 41.2 mmHg during exercise with balloon inflated. Similarly; for patient N3, we got a PAP of 36.4 mmHg during exercise with balloon inflated if we reduced the lumen diameter of muscular arteries by 35%. It might be due to vasoconstriction in response to a sudden increase in blood flow of high amplitude when the right lung was occluded during exercise.

For patients with mitral stenosis, the comparisons between our computed data and the experimental data are shown in **Table 5**. In our calculation, P_A = 0 cm $H_2O cm H_2O$, P_{pl} = -5 cm $H_2O cm H_2O$, and P_v equal to wedge pressure from experiments were used. In the column "Computed mean PAP", the same values of vessel diameters as in the calculation for normal subjects were used. The computed values

Table 4: Comparison between our and experimental data for normal subjects

Patient	Rest or exercise	Balloon	Blood flow (l/min)	Wedge pressure (mmHg)	Mean PAP from Experiment (mmHg)	Computed mean PAP (mmHg)
N1	R	I	7.3	10	22	25.0
	R	D	7.1	9	17	17.8
	E	I	10.2	12	27	30.0
	E	D	10.1	8	17	20.1
N2	R	I	6.5	13	27	25.5
	R	D	6.9	12	19	19.7
	E	I	10.5	20	42	34.8
	E	D	10.3	12	25	22.7
N3	R	I	5.8	9	24	22.0
	R	D	5.2	8	14	15.1
	E	I	10.7	10	36	29.7
	E	D	9.8	8	19	19.8

Note: R, rest; E, exercise; I, inflated; D, deflated; PAP, pulmonary arterial pressure.

Table 5: Comparison of computed data with experimental data for patients with mitral stenosis

Patient	R or E	Balloon	Blood flow (l/min)	Wedge pressure (mmHg)	Exp. mean PAP (mmHg)	Comp. mean PAP (mmHg)	Adjusted mean PAP (mmHg)	Vaso-constriction ratio (%)
M1	R	I	8.5	17	31	30.6	-	-
	R	D	8.9	16	21	24.3	-	-
	E	I	13.9	20	46	38.4	45.7	35
	E	D	14.4	15	26	27.7	-	-
M2	R	I	5.1	20	38	28.2	37.7	49
	R	D	5.8	17	27	22.5	26.8	44
	E	I	7.4	32	54	40.0	53.9	52
	E	D	6.6	27	37	31.4	36.6	47
M3	R	I	5.0	14	26	23.8	26.3	30
	R	D	4.6	14	18	19.0	-	-
	E	I	11.4	30	51	42.2	50.4	40
	E	D	10.5	29	40	35.4	39.8	40

Note: R, rest; E, exercise; I, inflated; D, deflated; PAP, pulmonary arterial pressure.

Table 6: Comparison between the computed and experimental data for patients with chronic bronchitis

Patient	R or E	Balloon	Blood flow (l/min)	Wedge pressure (mmHg)	Exp. mean PAP (mmHg)	Comp. mean PAP (mmHg)	Adjusted mean PAP (mmHg)	Vaso-constriction ratio (%)
C1	R	I	6.0	11	33	23.5	32.4	45
	R	D	5.6	11	30	17.7	29.5	56
	E	I	8.4	22	64	33.7	62.9	59
	E	D	8.9	20	52	27.3	52.0	62
C2	R	I	7.0	18	45	29.3	44.9	52
	R	D	7.4	17	39	23.8	38.5	57
	E	I	8.1	20	72	32.0	72.0	63
	E	D	8.3	19	64	26.1	63.1	67

Note: R, rest; E, exercise; I, inflated; D, deflated; PAP, pulmonary arterial pressure.

were much higher than the mean PAP values in normal subjects with similar blood flow, which could be explained as passive elevation of arterial pressure due to high wedge pressure in patients with mitral stenosis. However, the computed values were much less than their corresponding experimental results in most of the cases, indicating additional contributory factors other than passive backward transmission of the elevated left atrial pressure. Hence vasoconstriction of muscular arteries was assumed. The adjusted PAP value and ratio of vasoconstriction are shown in the last two columns. Our result was in general agreement with the founding by [Dev and Shrivastava (1991)] that pulmonary artery hypertension in patients with mitral stenosis was caused by two factors: (a) passive elevation of pressure resulting from increased wedge pressure, and (b) increasing pulmonary vascular resistance due to vasoconstriction. They also found that regression of the passive elevation in pulmonary artery pressure happened immediately after balloon mitral valvoplasty, while the increase in pulmonary artery pressure due to vasoconstriction regressed over the next week or so. Hermo-Weiler, Koizumi, Parker and Newman (1998) also proposed that left atrial hypertension could cause pulmonary vasoconstriction, which might be induced by mechanical vasodilation.

In **Table 5**, a general trend of increasing vasoconstriction with increasing blood flow was shown. This was in consistence with the viewpoint by Harris, Segel and Bishop (1968), e.g., when transmural pressure increased suddenly due to occlusion of the right lung, the resistance vessels of the left lung responded by an active muscular constriction.

For patients with chronic bronchitis, the comparisons between our computed data and the experimental data were shown in **Table 6**. The result of calculation using normal vessel diameter was shown in column "Computed mean PAP". In our calculation, P_A = 0 cm $H_2O cmH_2O$, P_{pl} = -5 cm $H_2O cmH_2O$ and P_v equal to wedge pressure from experiments were used. For all cases, the computed PAP was much lower than the experimental one. To get PAP value similar to experimental results, we simulated vasoconstriction of muscular arteries by reducing their lumen diameters. The results and corresponding ratio of vasoconstriction were shown in the last two columns of **Table 6**.

A strikingly different phenomenon in patients with chronic bronchitis was that pulmonary vascular resistance decreased significantly during occlusion of the right lung. Harris, Segel and Bishop (1968) stated that this was difficult to explain in terms of any alteration in the structure of the walls of vessels. If smooth muscle constriction was the only factor that contributes to the reduction of vessel lumen of the resistance arteries, vascular resistance should not fall during right lung occlusion since sudden increase in flow should result in stronger muscle contraction. A reasonable hypothesis would be that part of the vasoconstriction is caused by

high pressure in terminal air passages due to airway obstruction in patients with chronic bronchitis [Harris, Segel, Green and Giysket (1968)]. When the right lung is occluded, transmural pressure in the left lung increases suddenly and releases the compression upon arterioles caused by high airway pressure, thus the vessel lumen of resistance arteries are enlarged and vascular resistance decreased.

Compared to normal subjects and patients with mitral stenosis in **Table 6**, the effect of exercise in patients with chronic bronchitis was significant, which implied the resistance vessels had become narrowed during exercise [9]. In agreement with this finding, in our calculation, constriction ratio used for exercise was higher than those at rest, which could also be explained by increasing airway pressure that compressed resistance vessels.

The advantages of our continuum model are that it involves few assumptions and all parameters have true physiological meanings, which renders it capable for investigation of possible mechanisms behind specific kinds of pressure-flow relationship. Future work is needed in two aspects: (a) the measurement of elasticity data for arteries of order 4 and 5, arteries between orders 11 to 14, and veins between orders 9 to 15; and (b) additional experimental data are needed to validate and further develop the model, for example, data for extreme exercise, pulmonary vascular diseases, emphysema, etc.

In conclusion, a continuum model was introduced to analyze the pressure-flow relationship for steady flow in human pulmonary circulation. Our computed data showed general agreement with the experimental data for the normal subjects and the patients with mitral stenosis and chronic bronchitis in the literature. Our continuum model can be used to predict the changes of steady flow in human pulmonary circulation.

Acknowledgement: Wei Huang is supported by the Hong Kong Polytechnic University start-up fund 1-55-56-99EZ and initial grant A.55.37.PJ35.

References

1. Altman, P. L.; Dittmer, D. S. (eds) (1971): *Biological Handbook of Respiration and Circulation*. Bethesda, MA: Federation of American Societies for Experimental Biology, p. 110.

2. Chien, S. (2007): Mechanotransduction and endothelial cell homeostasis: the wisdom of the cell. *Am J Physiol Heart Circ Physiol.* 292: 1209-1224.

3. Dev, V.; Shrivastava, S. (1991): Time course of changes in pulmonary vascular resistance and the mechanism of regression of pulmonary arterial hy-

pertension after balloon mitral valvuloplasty. *Am J Cardiol* 67(5): 439-442.

4. Fowler, N. (1969): The Normal Pulmonary Arterial Pressure-Flow Relationships During Exercise. *Am J Med* 47(1): 1-6, 1969.

5. Fung, Y. C. (1972): Theoretical pulmonary microvascular impedance. *Ann Biomed Eng* 1: 221-245.

6. Fung, Y. C.; Sobin, S. S. (1969): Theory of sheet flow in lung alveoli. *J Appl Physiol* 26: 472-488.

7. Fung, Y. C.; Sobin, S. S. (1972): Pulmonary alveolar blood flow. *Circ Res* 30: 470-490.

8. Gan, R. Z.; Yen, R. T. (1994): Vascular impedance analysis in dog lung with detailed morphometric and elasticity data. *J Appl Physiol* 77(2): 706-717.

9. Gehr, P.; Bachofen, M.; Weibel, E. R. (1978): The normal human lung: ultrastructure and morphometric estimation of diffusion capacity. *Resp Physiol* 32(2): 121-140.

10. Harris, P.; Segel, N.; Bishop, J. M. (1968): The relation between pressure and flow in the pulmonary circulation in normal subjects and in patients with chronic bronchitis and mitral stenosis. *Cardiovasc Res* 2: 73-83.

11. Harris, P.; Segel, N.; Green, I.; Giysket, E. (1968): The influence of the airways resistance and alveolar pressure on the pulmonary vascular resistance in chronic bronchitis. *Cardiovasc Res* 2: 84-92.

12. Hermo-Weiler, C. I.; Koizumi, T.; Parker, R.; Newman, J. H. (1998): Pulmonary vasoconstriction induced by mitral valve obstruction in sheep. *J Appl Physiol* 85(5): 1655-1660.

13. Huang, W.; Yen, R. T.; McLaurine, M.; Bledsoe, G. (1996): Morphometry of the Human Pulmonary Vasculature. *J Appl Physiol* 81(5): 2123-2133.

14. Janicki, J. S.; Weber, K. T.; Likoff, M. J.; Fishman, A. P. (1985): The Pressure-Flow Response of the Pulmonary Circulation in Patients with Heart Failure and Pulmonary Vascular Disease. *Circulation* 72(6): 1270-1278.

15. Kussmaul, W. G.; Wieland, J. M.; Laskey, W. K. (1988): Pressure-Flow Relations in the Pulmonary Artery During Myocardial Ischaemia: Implications for Right Ventricular Function in Coronary Disease. *Cardiovasc Res* 22: 627-638.

16. Laskey, W. K.; Ferrari, V. A.; Palevsky, H. I; Kussmaul, W. G. (1993): Pulmonary Artery Hemodynamics in Primary Pulmonary Hypertension. *J Am Coll Cardiol* 21(2): 406-412.

17. Lee, J. S. (1969): Slow viscous flow in a lung alveoli model. *J Biomechanics* 2: 187-198.

18. Luchsinger, P.; Sachs, M.; Patel, D. (1962): Pressure-Radius Relationship in Large Blood Vessels of Man. *Circ Res* V XI: 885-888.

19. Seibold, H.; Wieshammer, S; Kress, P. (1988): Relation of Pressure and Flow of Pulmonary Circulation in Patients with Chronic Obstructive Pulmonary Disease. *Clin Physiol Biochem* 6: 29-35.

20. Singhal, S.; Henderson, R.; Horsfield, K.; Harding, K.; Cumming, G. (1973): Morphometry of the Human Pulmonary Arterial Tree. *Circ Res* 33: 190-197.

21. Sobin, S. S.; Fung, Y. C.; Lindal, R. G.; Tremer, H. M.; Clark, L. (1980): Topology of pulmonary arterioles, capillaries, and venules in the cat. *Microvasc Res* 19: 217-233.

22. Sobin, S. S.; Fung, Y. C.; Tremer, H. M.; Lindal, R. G. (1979): Distensibility of human pulmonary capillary blood vessels in the interalveolar septa. *Fed Proc* 38: 990.

23. Wagenvoort, C. A.; Wagenvoort, N. (1977): *Pathology of pulmonary hypertension.* New York: Wiley, p. 28.

24. Westerhof, N.; Stergiopulos, N.; Noble, M. I. M. (2004): *Snapshots of Hemodynamics*. Springer, New York, NY.

25. Yuan, J. X.J.; Garcia, J. G. N.; Hales, C. A.; Stuart, R.; Archer, S. L.; West, J. B. (eds.) (2010): *Textbook of Pulmonary Vascular Disease*. Springer, New York, NY.

26. Yen, R. T.; Fung, Y. C. (1973): Model experiment on apparent blood viscosity and hematocrit in pulmonary alveoli. *J Appl Physiol* 35: 510-517.

27. Yen, R. T.; Fung, Y. C.; Bingham, N. (1980): Elasticity of small pulmonary arteries in the cat. *J Biomech Eng* 102: 170-177.

28. Yen, R. T.; Sobin, S. S. (1988): Elasticity of Arterioles and Venules in Postmortem Human Lungs. *J Appl Physiol* 64: 611-619.

29. Yen, R. T.; Tai, D.; Rong, Z.; Zhang, B. (1990): Elasticity of Pulmonary Blood Vessels in Human Lungs. In: *Respiratory Biomechanics-Engineering Analysis of Structure and Function,* edited by Epstein and Ligas. New York: Springer-Verlag, p. 109-116.

30. Zhong, Z.; Dai, Y.; Mei, C. C.; Tong, P. (2002): A micromechanical theory of flow in pulmonary alveolar sheet. *Computer Modeling in Engineering & Sciences*, 3: 77-86.

31. Zhuang, F. Y.; Fung, Y. C.; Yen, R. T. (1983): Analysis of Blood Flow in Cat's Lung with Detailed Anatomical and Elasticity Data. *J Appl Physiol: Respirat Environ Exercise Physiol* 55(4): 1341-1348.